Netherlands Journal of Geosciences

www.cambridge.org/njg

Original Article

Cite this article: Trampert J, Benzi R, and Toschi F. Implications of the statistics of seismicity recorded within the Groningen gas field. *Netherlands Journal of Geosciences*, Volume 101, e9. https://doi.org/10.1017/njg.2022.8

Received: 20 December 2021
Revised: 11 March 2022
Accepted: 1 April 2022

Keywords:
induced seismicity; Groningen; earthquake statistics; elastic loading

Author for correspondence:
Jeannot Trampert, Email: j.a.trampert@uu.nl

CAMBRIDGE UNIVERSITY PRESS

Implications of the statistics of seismicity recorded within the Groningen gas field

Jeannot Trampert[1], Roberto Benzi[2] and Federico Toschi[3]

[1]Department of Earth Sciences, Utrecht University, Utrecht, The Netherlands; [2]Dipartimento di Fisica, Univ. degli Studi di Roma "Tor Vergata", Roma, Italy and [3]Department of Applied Physics, Eindhoven University of Technology, Eindhoven, The Netherlands

Abstract

We reanalysed the induced seismicity data from the Groningen gas reservoir. We used the well-maintained induced event catalogue of the KNMI. The distributions of seismic moments and interevent times show a power law behaviour over several decades, and we find that upon increasing the magnitude threshold, these distributions remained scale-invariant. Because of this scale-invariance, we can put a constraint on the average loading of the elastic energy within the reservoir, which upon reaching a critical value gives rise to the seismic events. We find that the elastic energy roughly increases proportional to time. We also propose a new machine learning approach for declustering the seismic events, separating correlated from independent events. We find that only few events are truly independent, i.e. exponentially distributed over time. There are also few aftershocks following an Omori-type power law. The bulk of events presents a Gamma distribution for interevent times. This gives us an indication that the rigidity in the reservoir is high, but whether this results in overall correlated events should be settled with physics-based arguments rather than statistical ones.

Introduction

The Groningen gas field is one of the largest in Europe and has been exploited since the 1960s. Since then, surface subsidence has been observed and induced seismicity slowly developed (van Thienen-Visser & Fokker, 2017; Dost et al., 2017). The connection between gas production, subsidence and seismicity is well-established (Van Eijs et al., 2006; Bierman et al., 2015) and a result of pore pressure loss due to gas extraction (Bourne et al., 2014). Compaction in the various geological units has been measured (Kole et al., 2017; Cannon & Cole, 2018; Kole et al., 2020) and linked to the observed seismic moment tensors (Bourne et al., 2014), which mostly show normal faulting (Willacy et al., 2019; Dost et al., 2020). Seismicity has slowly been building up over time, and with it, a very sophisticated and dense monitoring system (Dost et al., 2017). The correlation between the amount of gas production and the number of induced events can therefore be modelled reasonably well (Bourne et al., 2018).

Most earthquakes are small, but some reached a magnitude above 3. The fear is that even bigger events might cause serious damage to societal infrastructures in the area. Moment tensors are only estimated for the largest events (Willacy et al., 2019; Dost et al., 2020), which are well recorded across the monitoring network. Most seismic hazard analysis is based on point measurements of ground acceleration, maximum magnitude estimates and the frequency-magnitude relation. The latter is relatively well constrained, but the maximum magnitude is more uncertain (Dost et al., 2017).

While it is appealing to have simple models for earthquake generation, i.e. due to pore pressure loss in the thin reservoir layer (Bourne et al., 2014), it is not clear whether earthquakes occur randomly or present some space-time-magnitude correlations, resulting in earthquake clusters. A related question is whether all events are due to gas extraction, or if some are triggered by master events. Recent papers looked at this from various angles, using space-time declustering (Muntendam-Bos, 2020), nowcasting (Luginbuhl et al., 2018), non-stationary point processes (Post et al., 2021) and geomechanical modelling (Bourne et al., 2018; Candela et al., 2019). The estimates vary from very few to up to 27% correlated events. Most statistical analyses are based on stationarity, but the seismicity in Groningen clearly is not stationary: there is no sign of tectonic activity in the area, and seismicity slowly built up after gas production, which itself is irregular, and hopefully will stop some time after gas extraction ceases. Post et al. (2021) proposed a method to take this non-stationarity into account. Also, the number of recorded events is moderate, which means that robust statistical analysis is a challenge.

We will revisit the statistics of recorded events and analyse their scale-invariance. If size and interevent time probability distributions are scale-invariant, the rate of elastic energy accumulation can be inferred (Benzi et al., 2022), which is very important for geodynamic modelling in the area. We will also propose a method, based on machine learning, to extract information on

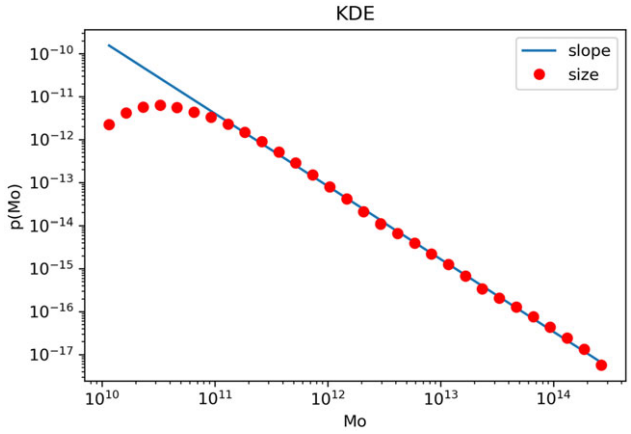

Fig. 1. Probability density of the seismic moment $p(M_0)$ for the Groningen catalogue using a cut-off magnitude of 0.5. The slope is 1.69.

the number of (un)correlated events in the catalogue. This model does not require any assumption on stationarity or point processes. It simply is a nonlinear inference method using the interevent time distribution as input.

Event statistics

In this study, we used the induced event file maintained by the KNMI (https://www.knmi.nl/kennis-en-datacentrum/dataset/aardbevingscatalogus) containing all induced earthquakes recorded since 1986 in the Netherlands. Not all induced events occurred within the Groningen gas field. We therefore restricted the catalogue to the Groningen events by imposing a simple latitude-longitude filter (53.0931-53.4909N and 6.5516-7.1048E). By using such a simple filter, we probably lost a few Groningen events and included a few from nearby fields, but this will not greatly influence our statistical arguments below. We also discarded all events before 2002 as the instrumentation was sparse before that date. Rather than looking at magnitudes, a more physically meaningful quantity is the seismic moment, which is proportional to seismic energy release. We therefore converted the local magnitudes m_l given by the KNMI into seismic moments using $\log_{10}M_0 = 1.5m + 9.105$, where M_0 is the seismic moment in [Nm] and m the moment magnitude (Hanks & Kanamori, 1979). Before doing so, we had to change local magnitudes m_l into moment magnitudes m using the expression in Dost et al. (2018). This expression is valid for local magnitudes between $0.5 \leq m_l \leq 3.6$. Restricting our catalogue further to events with a magnitude greater than 0.5 leaves us with 1372 events. We evaluated the probability distribution of the seismic moment using the Gaussian kernel density estimator from the SciPy statistics package (https://docs.scipy.org/doc/scipy/reference/generated/scipy.stats.gaussian_kde.html). We see (Fig. 1) that the probability density of the seismic moment presents a power law decay over four decades with a slope $\alpha = 1.69 \pm 0.01$ giving the power law $p(M_0) \propto M_0^{-\alpha}$. Using known relations from seismology (Ben-Zion, 2008), we can relate the slope of the seismic moment probability density to the Gutenberg–Richter law, which is cumulative, to give a Gutenberg-Richter slope $b = 1.04 \pm 0.02$. This is close to what has been reported elsewhere (Dost et al., 2017). It is worth noting that the reported b-values vary in different regions of the gas field, which is most likely due to changes in compaction (Bourne et al., 2014), or changes in magnitude of completeness used in various parts of the region.

Another statistic easily evaluated is that of interevent times. We follow Corral (2004) and estimate the probability density for interevent times, normalized by the average interevent time $< t_i >$, which is 5.06 days, using the same events. We observe (Fig. 3) that for longer times, the normalized interevent times follow a Gamma distribution $\gamma(0.64, 1.70)$ resulting in a negative slope of $\gamma = 0.36 \pm 0.02$ giving a power law behaviour $p(t_i/<t_i>) \propto (t_i/<t_i>)^{-\gamma}$ over two decades. This is slightly steeper than the values reported by Post et al. (2021), but close to the universal values of Corral (2004). At shorter times, the slope is much steeper and is thought to be due to the presence of aftershocks following an Omori-type behaviour (Corral, 2004). We find an Omori slope $p = 0.82 \pm 0.06$. Although on the low end, this is within the range of expected values (Utsu et al., 1995).

Both seismic moment and interevent times show a plateau at very low values of the respective variables. This is most likely due to the fact that the existing network, although dense, does not record all small events. There is a magnitude of completeness, above which all events are captured by the monitoring network. Dost et al. (2017) estimated this magnitude of completeness to be above 1.2 for the Groningen area. If we now repeat the statistical analysis for a magnitude cut-off of 1.3, we are left with 694 events. The new probability density functions can be seen in Figs. 2 and 4. We now find $\alpha = 1.66 \pm 0.02$ and $\gamma = 0.31 \pm 0.05$. The uncertainty in the slope of the intervent time curve is significantly larger, due to the dip at 10^{-3}, which is likely due to the significantly smaller number of events using this higher cut-off. Within the uncertainties though, and certainly within two standard deviations, the slopes are the same. Introducing a magnitude of completeness eliminates the plateau in Fig. 2, while the interevent time curve remains largely unchanged (the Omori slope is now $p = 0.87 \pm 0.05$). The average interevent time $< t_i >$ for this higher magnigtude cut-off is 8.87 days. We checked that for other magnitude cut-offs, the power law parts of $p(M_0)$ and $p(t_i/<t_i>)$ remained the same within the uncertainties, indicating that they are indeed scale-invariant.

Implications of the scale-invariance

In Benzi et al. (2022), we showed that if $p(M_0)$ and $p(t_i/<t_i>)$ are scale-invariant, α and γ are related for two specific cases of energy loading in various systems. Let us generalise this result. Assume that an earthquake releases the elastic energy that has been stored in the system over time. After the earthquake released it, energy will start being stored again and we assume that it grows as some power of the normalized interevent time. The released energy is proportional to the seismic moment (Ben-Zion, 2008). We can then consider a new random variable $X = \frac{E_{\text{stored}}}{E_{\text{released}}} = \frac{(t_i/<t_i>)^{\epsilon}}{M_0}$. This constant power ϵ can be interpreted as the average over the considered time span 2002–2021 and does not model possible changes due to variations in the volume of gas extraction over the same time span. Indeed Bierman et al. (2015) analysed the rates of earthquakes in Groningen and found a possible correlation with changes in gas extraction for events of magnitude lower than 1.5. Using the ratio distribution rule, $p(t_i/<t_i>) \propto (t_i/<t_i>)^{-\gamma}$ and $p(M_0) \propto M_0^{-\alpha}$, the probability density for X is

$$p(X) = X^{\frac{1-\gamma}{\epsilon}-1} \int M_0^{\frac{1-\gamma}{\epsilon}-\alpha} dM_0, \qquad (1)$$

https://doi.org/10.1017/njg.2022.8 Published online by Cambridge University Press

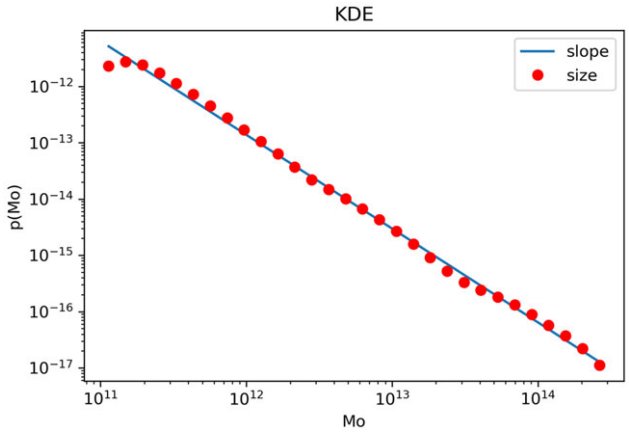

Fig. 2. Probability density of the seismic moment $p(M_0)$ for the Groningen catalogue using a cut-off magnitude 1.3. The slope is 1.66.

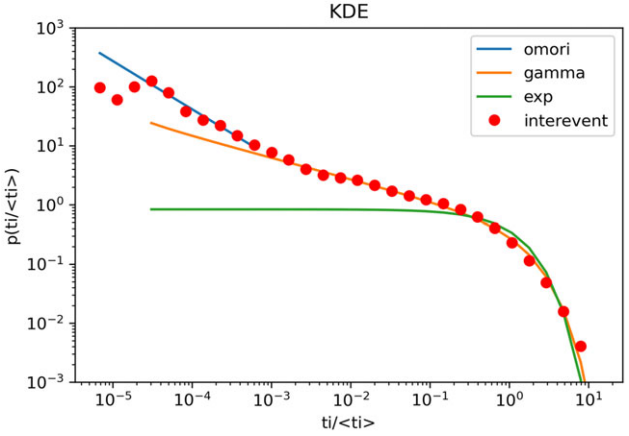

Fig. 3. Probability density of the normalised interevent time $p(t_i/<t_i>)$ for the Groningen catalogue using a cut-off magnitude of 0.5. The Omori slope is 0.82, and the Gamma slope is 0.36.

where the integration is over the part where the seismic moment shows a power law. Now let us consider the scale transformation

$$M_0 \rightarrow \lambda M_0 \tag{2}$$

We then find that

$$p(X) \rightarrow \lambda^{\frac{1}{\varepsilon}-\frac{\gamma}{\varepsilon}-\alpha+1} p(X). \tag{3}$$

Since both $p(M_0)$ and $p(t_i/<t_i>)$ are scale-invariant, $p(X)$ is too. This implies that the exponent of λ has to be 0 and

$$\gamma + \varepsilon\alpha = 1 + \varepsilon. \tag{4}$$

Using the measured slopes for the seismic moment and interevent time above, we find that for a magnitude cut-off of 0.5, $\epsilon = 0.93 \pm 0.03$and $\epsilon = 1.05 \pm 0.04$ for events above the magnitude cut-off of 1.3. For all practical purposes, we infer that the elastic energy within the Groningen gas reservoir roughly increases linearly with time until a new event occurs, i.e. $\epsilon \approx 1$. It is remarkable that this loading is very similar to that of tectonic earthquakes (Benzi et al., 2022).

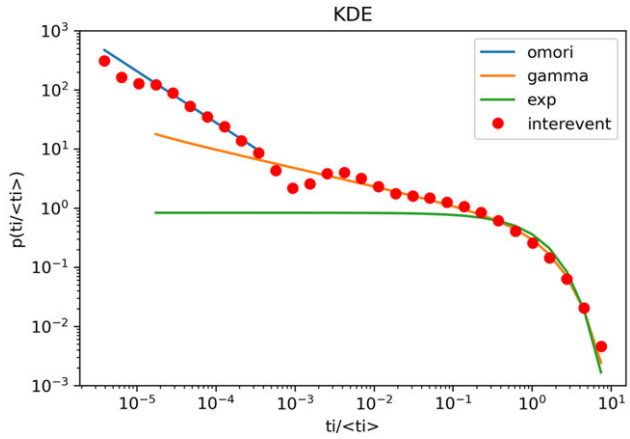

Fig. 4. Probability density of the normalised interevent time $p(t_i/<t_i>)$ for the Groningen catalogue using a cut-off magnitude of 1.3. The Omori slope is 0.87, and the Gamma slope is 0.31.

Modelling interevent time using gradient boosted trees

Except for very short interevent times, $p(t_i/<t_i>)$ closely follows a Gamma distribution (Figs. 3 or 4). A Gamma distribution could be an indication of some correlation between magnitude, space and time (Corral, 2005). Furthermore, a clear Omori slope is present at short interevent times. Another common assumption is that some events are truly independent and follow a Poisson process, resulting in an exponential distribution. An important question therefore is how many aftershocks are following Omori's power law, how many events a Gamma distribution and how many independent events an exponential distribution in the Groningen catalogue. Without explicitly distinguishing between aftershocks (Omori) and otherwise correlated events, the amount of correlated events was estimated to be between a few percent up to 27% (Luginbuhl et al., 2018; Bourne et al., 2018; Candela et al., 2019; Muntendam-Bos, 2020; Post et al., 2021). Most of the studies based on statistics assume stationarity to perform some form of declustering, except for the latter. We propose a machine learning route to interpret the interevent time distribution directly without any assumptions, except that the observed distribution is a mixture of Omori distributed, Gamma distributed and exponentially distributed events.

We generated 10^5 samples from a power law, 10^5 samples from a Gamma distribution, whose coefficients have been taken from the interevent times above, and 10^5 samples from an exponential distribution. We then uniformly draw a random number $n_g \in [0,1]$ representing the fraction of samples from the Gamma distribution and $n_e \in [0,1]$ representing the fraction of samples from the exponential distribution. If $n_g + n_e \leq 1$, then $n_p = 1 - n_g - n_e$ is the fraction of power law samples. If however, $n_g + n_e > 1$, we assume that the interevent distribution is dominated by either the Gamma or the exponential distribution, i.e. if $n_g > n_e$, $n_e = 0$ and $n_p = 1 - n_g$, else if $n_g < n_e$, $n_g = 0$ and $n_p = 1 - n_e$. We then generate a set of in total 10^4 samples randomly composed of a fraction n_g Gamma distributed samples, a fraction n_e exponentially distributed samples and a fraction n_p power law distributed samples. Similar to the Groningen event data, we estimate the probability density for this set using a Gaussian kernel density estimator. The aim is to infer the fractions n_g, n_e and n_p directly from the probability density curve. To solve this regression problem, we used gradient boosting trees (Friedman, 2001) implemented by the Python machine learning package (https://scikit-learn.org/stable/

https://doi.org/10.1017/njg.2022.8 Published online by Cambridge University Press

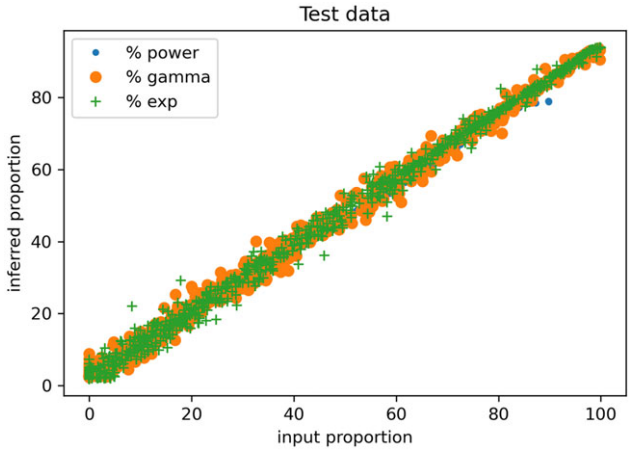

Fig. 5. Performance of the gradient boosting random forest for a data set of 1000 unseen distributions.

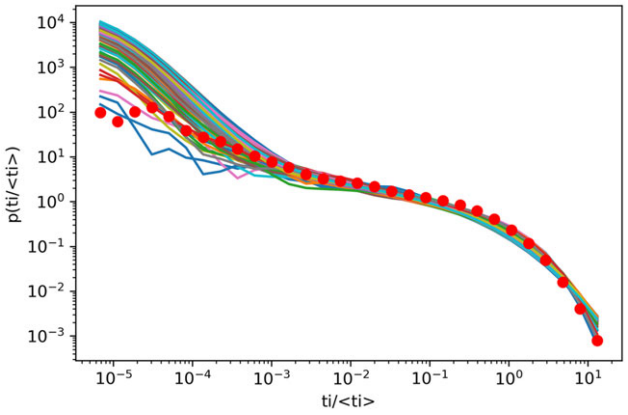

Fig. 6. Hundred realizations of the interevent times using the inferred proportions of the Omori, Gamma and exponential distributions within their standard deviation. The observed interevent time distribution is shown by red dots and coresponds to a cut-off magnitude of 0.5. Note that the narrow plateau at very short times has not been included in the modelling.

modules/generated/sklearn.ensemble.GradientBoostingRegressor.html). We created a training set of 5000 such probability density curves, which serve as input to the gradient boosting regressor and the fractions n_g, n_e and n_p are the target.

Splitting the training set into 80% training data and 20% test data, we show the performance of the trained gradient boosting regressor on the test data not previously seen by the regressor model (Fig. 5). The output points nicely fall on the diagonal, indication that the model has successfully learned the sample fractions from the input data. Another indication that the learning was successful is that the R^2-score for the test data is 0.98, similar to the score for the training data. We experimented with increasing the training set and slightly changing the parameters of the input distributions, but results remained similar. As can be seen in Fig. 5, the model is not perfect and there is some spread around the diagonal, which will result in some uncertainty in the inference from the observed interevent time distribution. We can directly use this spread to infer the uncertainty on our inference by estimating the standard deviation of the points around the diagonal.

Regardless of the cut-off magnitude, we find $n_p = 0.03 \pm 0.02$, $n_g = 0.92 \pm 0.03$ and $n_e = 0.03 \pm 0.03$. It is not surprising that this inference is independent of the magnitude cut-off as the interevent time distribution is scale-invariant. Figure 6 shows that indeed the inferred fractions closely match the observed interevent time distribution, except for the plateau at the shortest times, which has not been modelled.

Concluding remarks

We reanalysed the Groningen event catalogue and estimated the distributions for seismic moment and interevent times. Upon increasing the cut-off magnitude in the catalogue, we showed that both distributions are scale-invariant. This scale-invariance implies that the dominant slopes in the seismic moment and interevent time distributions are related to the time evolution of the elastic energy loading in the system. We found that $E_{\text{stored}} \propto (t_i / < t_i >)$. The interevent time distribution indicates that most events are Gamma distributed. To gain more insight, we trained a gradient boosting regressor to infer the proportion of aftershocks (following an Omori power law), the proportion of events following a Gamma distribution and the proportion of independent events following an exponential distribution. Most events follow a Gamma distribution and very few an Omori power law or an exponential distribution.

The elastic energy that is stored over time, until a seismic event releases it, can be written as E, where σ is the effective stress and ϵ the vertical strain (Bourne & Oates, 2017). Most events are located within the gas reservoir (Dost et al., 2017) and thus the temporal evolution of the stored energy, which we measured, also relates to the reservoir. Measurements of vertical strain in the reservoir using radioactive markers or distributed strain sensing show that the vertical strain increases proportional to time (Kole et al., 2017; Cannon & Cole, 2018; Kole et al., 2020), we therefore deduce that the effective stress is roughly constant. This is similar to tectonic earthquakes where it is commonly assumed that apparent stress is constant (Madariaga, 2011). Bourne & Oates showed that the effective stress is $\sigma = C\Delta P$ where C is a factor, which is a function of the elastic constants and the Biot coefficient and ΔP is the pressure depletion in the reservoir. The pressure depletion $\Delta P \propto t$ (https://www.nam.nl/feiten-en-cijfers/gasdruk.html) and hence $C \propto t^{-1}$. We suggest that these loading rules should be used in future geodynamic modelling of the reservoir.

Recently, there has been some interest in declustering the Groningen catalogue and estimate the number of correlated events using various techniques (Luginbuhl et al., 2018; Bourne et al., 2018; Candela et al., 2019; Muntendam-Bos, 2020; Post et al., 2021). We proposed a machine learning approach using the interevent time distribution as input to infer the proportion of aftershocks, the proportion of events following a Gamma distribution and the proportion of independent events. Existing estimates of correlated events (mostly assumed to be aftershocks) vary from a few percent to up to 27%. We find that the proportion of aftershocks in the Groningen catalogue following an Omori-type law is most likely less than 7%. Similarly, we find that the most likely range of truly independent events, following an exponential distribution, to be between 0 and 9%. Both of these ranges are 95% confidence levels or 2 standard deviations. This leaves the bulk of events following a Gamma distribution. The question is if those events are correlated in some way or not. From a statistical point of view, assuming stationarity, the shape parameter of the Gamma distribution can be thought of as the ratio of independent over total events. Post et al. (2021) modified this relation to incorporate non-stationarity. These statistical arguments do not contain any

https://doi.org/10.1017/njg.2022.8 Published online by Cambridge University Press

physical insight though. From a material science point of view, we know that many systems presenting avalanche dynamics show interevent time statistics evolving from exponential to Gamma distributions upon increasing compaction, confining pressure or rigidity (Kumar et al., 2020). Kumar et al. (2020) also indirectly showed that, in case these interevent times are Gamma distributed, the systems presented some space-time correlations. Future work should therefore try and unravel the exact physics processes, which give rise to these correlations, and how they relate to gas extraction and hence compaction in the reservoir and try and link this understanding to the occurrence and forecasting of seismicity.

Acknowledgements. Two anonymous reviewers provided constructive comments, which are greatfully acknowledged. We thank Elmer Ruigrok who provided suggestions for filtering KNMI's induced event catalogue and Hanneke Paulssen who provided constructive comments on an earlier version of this paper. The research leading to these results has received funding from the research programme DeepNL of the Dutch Research Council (NWO) under project number DeepNL.2018.033.

Competing interests. The authors declare none.

References

Ben-Zion, Y., 2008. Collective behavior of earthquakes and faults: Continuum-discrete transitions, progressive evolutionary changes, and different dynamic regimes. Reviews of Geophysics **46**(4): RG4006.

Benzi, R., Castaldi, I., Toschi, F. & Trampert, J., 2022. Self-similar properties of avalanche statistics in a simple turbulent model. Philosophical Transactions A **380**(2218): 20210074.

Bierman, S., Paleja, R. & Jones, M., 2015. Statistical methodology for investigating seasonal variation in rates of earthquake occurrence in the Groningen field. Shell and NAM BV, SR.15.13132 (Amsterdam).

Bourne, S. & Oates, S., 2017. Extreme threshold failures with a heterogeneous elastic thin sheet and spatio-temporal development of induced seismicity within the Groningen gas field. Journal of Geophysical Research: Solid Earth **122**: 10299–10320. doi: 10.1002/2017/JB014356.

Bourne, S., Oates, S., Elk, J.v & Doornhof, D., 2014. A seismological model for earthquakes induced by fluid extraction from a subsurface reservoir. Journal of Geophysical Research: Solid Earth **119**(12): 8991–9015.

Bourne, S., Oates, S. & Elk, J.v, 2018. The exponential rise of induced seismicity with increasing stress levels in the groningen gas field and its implications for controlling seismic risk. Geophysical Journal International **213**(3): 1693–1700.

Candela, T., Osinga, S., Ampuero, J.-P., Wassing, B., Pluymaekers, M., Fokker, P.A., van Wees, J.-D., de Waal, H.A. & Muntendam-Bos, A.G., 2019. Depletion-induced seismicity at the groningen gas field: coulomb rate-and-state models including differential compaction effect. Journal of Geophysical Research: Solid Earth **124**(7): 7081–7104.

Cannon, M. & Cole, P.R., 2018. The first year of distributed strain sensing (DSS) - Monitoring in the Groningen gas field. Shell and NAM BV, SR.17.00934 (Amsterdam).

Corral, A., 2004. Long-term clustering, scaling, and universality in the temporal occurrence of earthquakes. Physical Review Letters **92**(10): 108501.

Corral, A., 2005. Renormailzation-group transformations and correlations of seismicity. Physical Review Letters **95**(2): 028501.

Dost, B., Ruigrok, E. & Spetzler, J., 2017. Development of seismicity and probabilistic seismic hazard assessment for the Groningen gas field. Netherlands Journal of Geosciences **96**(5): s235–s245. doi: 10.1017/njg.2017.20.

Dost, B., Edwards, B. & Bommer, J.J., 2018. The relationship between m and m_l: A review and application to induced seismicity in the Groningen gas field, the Netherlands. Seismological Research Letters **89**(3): 1062–1074.

Dost, B., van Stiphout, A., Kühn, D., Kortekaas, M., Riogrok, E. & Heinmann, S., 2020. Probabilistic moment tensor inversion for hydrocarbon-induced seismicity in the groningen gas field, the netherlands, part 2: application. Bulletin of the Seismological Society of America **110**(5): 2112–2123.

Friedman, J., 2001. Greedy function approximation: a gradient boosting machine. The Annals of Statistics **29**(5): 1189–1232.

Hanks, T. & Kanamori, H., 1979. A moment magnitude scale. Journal of Geophysical Research **84**(B5): 2348–2350.

Kole, P., Cannon, M., Doornhof, D. & van Elk, J., 2017. First year of distributed strain sensing in the Groningen field. *In:* EAGE/DGG Workshop on Fibre Optic Technology in Geophysics, Extended abstracts, Fr SR P05.

Kole, P., Cannon, M., Tomic, J. & Bierman, S., 2020. Analysis of and learnings from the first four years of in-situ strain data in Zeerijp-3A. Shell and NAM BV, EP201908210907 (Amsterdam).

Kumar, P., Korkolis, E., Benzi, R., Denisov, D., Niemeijer, A., Schall, P., Toschi, F. & Trampert, J., 2020. On interevent time distributions of avalanche dynamics. Scientific Reports **10**(1): 626.

Luginbuhl, M., Rundle, J. & Turcote, D., 2018. Natural time and nowcasting induced seismicity at the Groningen gas field in the Netherlands. Geophysical Journal International **215**(2): 753–759.

Madariaga, R., 2011. Earthquake scaling laws. *In:* Meyer, R.A. (ed.): Extreme environmental events. Springer (New York): 364–383.

Muntendam-Bos, A., 2020. Clustering characteristics of gas-extraction induced seismicity in the Groningen gas field. Geophysical Journal International **221**(2): 879–892.

Post, R., Michels, M., Ampuero, J.-P., Candela, T., Fokker, P., van Wees, J.-D., van der Hofstad, R. & van den Heuvel, E., 2021. Interevent-time distribution and aftershock frequency in non-stationary induced seismicity. Scientific Reports **11**(1): 3540.

Utsu, T., Ogata, Y. & Matsu'ura, S., 1995. The centenary of the omori formula for a decay of aftershock activity. Journal of Physics of the Earth **43**(1): 1–33.

Van Eijs, R., Mulders, F., Nepveu, M., Kenter, C. & Scheffers, B., 2006. Correlation between hydrocarbon reservoir properties and induced seismicity in the Netherlands. Engineering Geology **84**(3): 99–111.

van Thienen-Visser, K. & Fokker, P.A., 2017. The future of subsidence modelling: compaction and subsidence due to gas depletion of the Groningen gas field in the Netherlands. Netherlands Journal of Geosciences **96**(5): 1–12.

Willacy, C., van Dedem, E., Minisini, S., Li, J., Blokland, J.-W., Das, I. & Droujinine, A., 2019. Full-waveform event location and moment tensor inversion for induced seismicity. Geophysics **84**(2): KS39–KS57.